Journal of Catalysis **192,** 18–28 (2000)
doi:10.1006/jcat.2000.2822, available online at http://www.idealibrary.com on IDEAL®

Structural Characteristics and Reactivity Properties of Highly Dispersed Al_2O_3/SiO_2 and $V_2O_5/Al_2O_3/SiO_2$ Catalysts

Xingtao Gao and Israel E. Wachs

Department of Chemistry and Chemical Engineering, Zettlemoyer Center for Surface Studies, Lehigh University, 7 Asa Drive, Bethlehem, Pennsylvania 18015
E-mail: xig2@lehigh.edu, iew0@lehigh.edu.

Received July 19, 1999; revised January 14, 2000; accepted January 24, 2000

Highly dispersed Al_2O_3/SiO_2 and $V_2O_5/Al_2O_3/SiO_2$ catalysts under various conditions (e.g., hydration, dehydration, and methanol chemisorption) were investigated by *in situ* **Raman and UV–vis-NIR diffuse reflectance spectroscopies. Temperature-programmed reduction and methanol oxidation were employed as chemical probe reactions to examine the reducibility and reactivity properties of these catalysts. The spectroscopic results revealed that the surface vanadium oxide species on the Al_2O_3/SiO_2 supports are predominantly isolated VO_4 units [O═V(O–Support)$_3$] in the dehydrated state. The surface vanadium oxide species preferentially interact with the aluminum oxide species on the silica surface. Consequently, the reduction behavior of the surface vanadium oxide species is closer to that of V_2O_5/Al_2O_3 at higher alumina loading. Furthermore, the turnover frequency of the surface VO_4 species on Al_2O_3/SiO_2 for methanol oxidation to redox products (formaldehyde, methyl formate, and dimethoxy methane) increases by an order of magnitude relative to the V_2O_5/SiO_2 catalysts and is comparable to that of the V_2O_5/Al_2O_3 catalysts. It is concluded that the substitution of the Si(IV)–O^- by the less electronegative Al(III)–O^- ligands for the isolated VO_4 units is responsible for the enhanced reactivity of the surface V cations.** © 2000 Academic Press

Key Words: **Al_2O_3/SiO_2 and $V_2O_5/Al_2O_3/SiO_2$ supported metal oxides; surface structure; methanol oxidation; temperature-programmed reduction (TPR); Raman spectroscopy; UV–vis-NIR diffuse reflectance spectroscopy (DRS).**

INTRODUCTION

Amorphous alumina–silica catalysts are among the most widely used solid acid catalysts in the oil and chemical industries and are largely applied for isomerization of olefins, paraffins, and alkyl aromatics, alkylation of aromatics with alcohols and olefins, and olefins oligomerization and catalytic cracking (1). Amorphous alumina–silica can also be used as supports or catalyst components for other reactions, such as ammoxidation of 3-picoline (V_2O_5/Al_2O_3–SiO_2) (2), combustion of methane (Pd–Al_2O_3/SiO_2) (3), denitrogenation of nitrogen-containing heteroaromatic compounds (Al_2O_3–SiO_2 and Mo/Al_2O_3–SiO_2) (4), and dimerization and oligomerization of olefins (NiO–Al_2O_3/SiO_2) (5). The catalytic properties of amorphous alumina–silica catalysts are usually correlated with the Brönsted acidity that is located on the Al–OH–Si bridging bonds.

The interaction of alumina with silica either in the silica matrices or at their interface is expected to generate new active sites as a result of the chemical bonding between Al(III) and Si(IV) cations. Silica deposited on alumina generates Brönsted acidity (6–8), which is stable upon thermal treatment up to 1493 K (9). These silica-on-alumina monolayer catalysts were found to display high-catalytic activities for 2-butanol dehydration, *m*-xylene isomerization, cumene cracking, and *n*-heptane cracking that are comparable to commercial amorphous silica–aluminas (6). It is, thus, intriguing that alumina-modified silica would display similar catalytic behaviors. So far, no systematic and fundamental investigation has been performed on highly dispersed alumina on silica catalytic materials.

In the present study, a very reactive Al *sec*-butoxide was used to prepare the highly dispersed Al_2O_3/SiO_2 supported oxides. Highly dispersed metal oxides on SiO_2 are often prepared by the surface reaction of Si–OH hydroxyls with highly reactive H-sequestering reagents since the surface Si–OH hydroxyls usually act as the adsorption/reactive sites due to their hydrophilic nature (10). The dispersion and possible surface structure of dispersed aluminum oxide species on silica were investigated by Raman spectroscopy, X-ray photoelectron spectroscopy (XPS), and UV–vis-NIR diffuse reflectance spectroscopy (DRS). The catalytic properties of the highly dispersed Al_2O_3/SiO_2 catalysts were also examined using methanol oxidation as a probe reaction.

Furthermore, the highly dispersed Al_2O_3/SiO_2 samples were used as support materials for vanadium oxide. Thus, a series of highly dispersed $V_2O_5/Al_2O_3/SiO_2$ catalysts were prepared as model catalysts to understand the interfacial interactions between surface vanadium oxide and surface aluminum oxide on silica. The molecular structures of the highly dispersed $V_2O_5/Al_2O_3/SiO_2$ catalysts under various conditions (e.g., hydration and dehydration) were extensively investigated with *in situ* Raman spectroscopy and UV–vis-NIR DRS. Methanol oxidation was used to

0021-9517/00 $35.00

examine the catalytic properties of the $V_2O_5/Al_2O_3/SiO_2$ catalysts, and temperature-programmed reduction (TPR) was used to examine their redox properties. The results from these studies allow us to establish the fundamental relationships between the structural characteristics and the reactivity/selectivity properties of this catalyst system and to provide a better understanding about how to molecularly engineer supported metal oxide catalysts by modifying the support material.

EXPERIMENTAL

1. Catalyst Preparation

The silica support was Cabosil EH-5 ($S_{BET} = 332$ m^2/g). The Al_2O_3/SiO_2 supported oxides were prepared by the incipient-wetness impregnation of isobutanol solutions of aluminum *sec*-butoxide (Alfa-Aesar 95% purity). The preparation was performed inside a glove box with continuously flowing N_2. The SiO_2 support was initially dried at 120°C to remove the physisorbed water before impregnation. After impregnation at room temperature, the samples were kept inside the glove box with flowing N_2 overnight. The samples were subsequently dried at 120°C in flowing N_2 for 1 h and calcined at 500°C in flowing air for 4 h. The catalysts were denoted as x wt% Al_2O_3/SiO_2 ($x = 1, 3, 5, 10$). The BET surface areas of the Al_2O_3/SiO_2 samples were measured by nitrogen adsorption/desorption isotherms on a Micromeritics ASAP 2000.

The supported vanadia catalysts were prepared by the incipient-wetness impregnation of isopropanol solutions of vanadium isopropoxide ($VO(O\text{-}Pr^i)_3$, Alfa-Aesar 97% purity) with supports. The preparation procedure is the same as the previous one before calcination. The samples obtained after impregnation were dried in flowing N_2 at 120°C for 1 h and 300°C for 1 h. Then, the $V_2O_5/Al_2O_3/SiO_2$ samples were calcined in flowing air at 300°C for 1 h and 500°C for 2 h, while the V_2O_5/SiO_2 and V_2O_5/Al_2O_3 samples were calcined in flowing air at 300°C for 1 h and 450°C for 2 h.

2. Raman Spectroscopy

The Raman spectra were obtained with the 514.5-nm line of an Ar^+ ion laser (Spectra Physics, Model 164). The scattered radiation from the sample was directed into an OMA III (Princeton Applied Research, Model 1463) optical multichannel analyzer with a photodiode array cooled thermoelectrically to −35°C. The laser power used at the source is 15–30 mW, and the acquisition time is 30 s/per scan with a total of 25 scans for each sample. The samples were pressed into self-supporting wafers. The Raman spectra of the hydrated samples were collected during rotation of the samples under ambient conditions. The Raman spectra of the dehydrated samples were recorded at room temperature after the samples were heated in flowing O_2 at 450–500°C for 1 h in a stationary quartz cell.

3. X-ray Photoelectron Spectroscopy (XPS)

XPS spectra were collected with a Fisons ESCALAB 200R electron spectrometer equipped with a hemispherical electron analyzer and an Mg$K\alpha$ X-ray source ($h\nu = 1253.6$ eV) powered at 120 W. A PDP 11/05 computer from DEC was used for collecting and analyzing the spectra. All samples were outgassed at 200°C before XPS analysis. The binding energies (BE) were referenced to Si 2p (BE = 103.4 eV) with an accuracy of ±0.2 eV. The atomic concentration ratios were calculated by correcting the intensity ratios with theoretical sensitivity factors proposed by the manufacturer.

4. UV–Vis-NIR Diffuse Reflectance Spectroscopy (DRS)

DRS spectra in the range of 200–2200 nm were taken on a Varian Cary 5 UV–vis-NIR spectrophotometer. The spectra were recorded against a halon white reflectance standard as the baseline. The computer processing of the spectra with Bio-Rad Win-IR software consisted of calculation of the Kubelka–Munk function ($F(R_\infty)$) from the absorbance. Samples were loaded in a quartz flow cell with a Suprasil window. After each treatment, the quartz cell was quickly sealed off and cooled down to room temperature for DRS measurements. The hydrated spectra were obtained under ambient conditions. The dehydrated spectra were obtained after the samples were calcined at 500°C in flowing O_2/He for 1 h. The DRS spectra for methanol chemisorption were recorded after the dehydrated sample was contacted with a gaseous mixture of CH_3OH/O_2/He (4 mol% CH_3OH in the saturated gaseous mixture) at various temperatures for 30 min.

5. Temperature-Programmed Reduction (TPR)

TPR experiments were carried out in an AMI-100 system (Zeton Altamira Instruments). The experimental setup and procedures have been described in detail elsewhere (11). After the first TPR run, some reduced samples were then reoxidized at 500°C in flowing dry air for 1 h, and the reoxidized samples were used for the second TPR run to examine the stability of the catalyst sample during the redox cycle.

6. Methanol Oxidation

Methanol oxidation was used to examine the reactivity/selectivity of Al_2O_3/SiO_2 and $V_2O_5/Al_2O_3/SiO_2$ catalysts. The reactant gas mixture of CH_3OH/O_2/He, molar ratio of ~6/13/81, was used with a total flow rate of 100 ml/min. The experimental setup and procedures have been described in detail elsewhere (11).

TABLE 1

Surface Areas and XPS Surface Analysis of the Al_2O_3/SiO_2 Samples

Sample	Surface area (m^2/g)	Al 2*p* (eV)	O 1*s* (eV)	Al/Si surface atomic ratio
SiO_2	332	—	533.0	0.000
1% Al_2O_3/SiO_2	304	75.1	532.9	0.016
3% Al_2O_3/SiO_2	270	75.0	532.9	0.056
5% Al_2O_3/SiO_2	253	75.0	532.9	0.079
10% Al_2O_3/SiO_2	220	74.8	533.0	0.164

RESULTS

1. *Surface Areas and XPS Surface Analysis of the Al_2O_3/SiO_2 Samples*

The surface areas of the Al_2O_3/SiO_2 samples decrease systematically with increasing alumina loading; see Table 1. The XPS surface Al/Si atomic ratios and binding energy (BE) values of Al 2*p* and O 1*s* for the dehydrated Al_2O_3/SiO_2 samples are also listed in Table 1. The Al/Si surface ratios appear to be linearly correlated with the alumina concentration, as seen in Fig. 1, which suggests that the aluminum oxide species may be highly dispersed on the silica surface. The BE of O 1*s* for these Al_2O_3/SiO_2 samples keeps almost constant at ~532.9 eV, whereas the BE of Al 2*p* slightly decreases from 75.1 to 74.8 eV as the loading increases from 1% to 10% Al_2O_3.

2. *Raman Spectroscopy*

The Raman spectrum of the hydrated 10% Al_2O_3/SiO_2 sample is shown in Fig. 2. The silica support under hydrated and dehydrated conditions possesses the same Raman features at ~410, ~487, 607, 802, and ~976 cm^{-1}. No significant spectral change can be seen upon the deposition of aluminum oxide species onto the silica surface, with exception of the 976-cm^{-1} band due to the Si–OH stretching vibration (12). The 976-cm^{-1} band disappears almost completely after 10% Al_2O_3 loading on silica, indicative of the consumption of the Si–OH hydroxyls by deposition of aluminum oxide species. Unfortunately, it is not possible to obtain the Raman spectra for the dehydrated Al_2O_3/SiO_2 samples since extremely high fluorescence is detected on these samples.

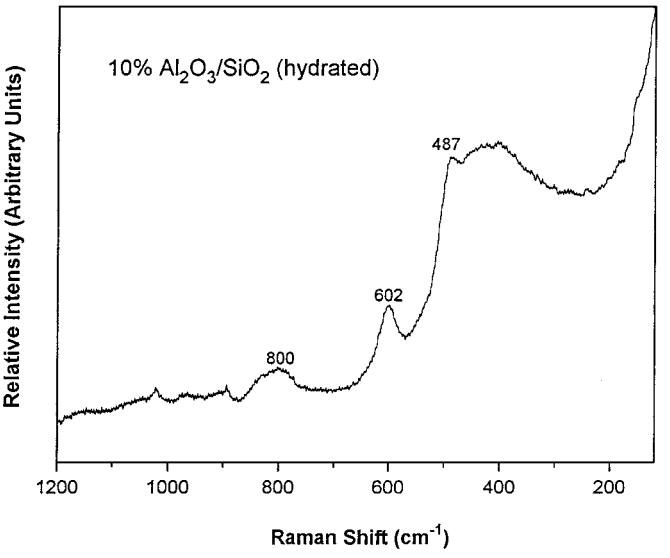

FIG. 2. Raman spectrum of the hydrated 10% Al_2O_3/SiO_2 sample.

The Raman spectra of the dehydrated 10% V_2O_5 on 0–10% Al_2O_3/SiO_2 supports are compared in Fig. 3. No V_2O_5 crystallites are present on these samples since Raman bands at 994, 697, 284, and 144 cm^{-1} due to crystalline V_2O_5 are not detected. The dehydrated 10% V_2O_5/SiO_2 sample possesses a Raman band at 1041 cm^{-1} from the terminal V=O vibration of the isolated VO_4 species and bands at 1072, 915, and 481 cm^{-1} due to silica vibrations (13). Modification of silica by the aluminum oxide species does not change significantly the major spectral feature of the isolated VO_4 species on silica. Increasing alumina loading slightly shifts the V=O stretching vibration to lower wavenumbers from 1041 to 1035 cm^{-1}, whereas the growth of the Raman band at 915–925 cm^{-1} is very minor with alumina loading up to 10% Al_2O_3. The 915- to 925-cm^{-1} band is usually associated with the surface polymeric vanadia species; however, no apparent additional bands appear at 200–300 cm^{-1} due to the V–O–V bending mode of the polymeric vanadia species (14). For the dehydrated 1% V_2O_5/Al_2O_3 sample, where the isolated VO_4 species are dominant, a broad Raman band observed at 840–940 cm^{-1} was assigned to the VO_3 stretching functionalities (14). It is

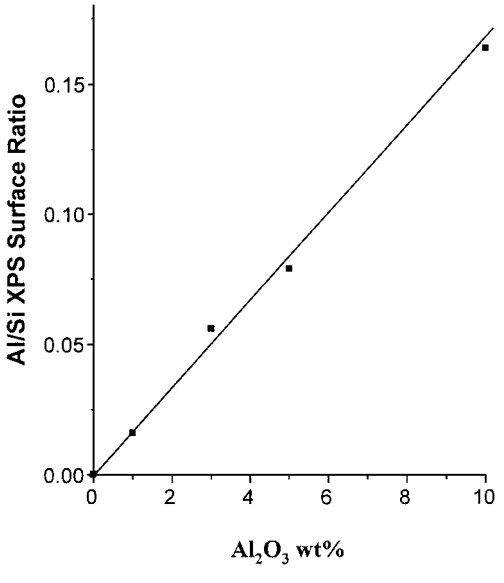

FIG. 1. Al/Si XPS surface atomic ratio as a function of the Al_2O_3 loading on silica.

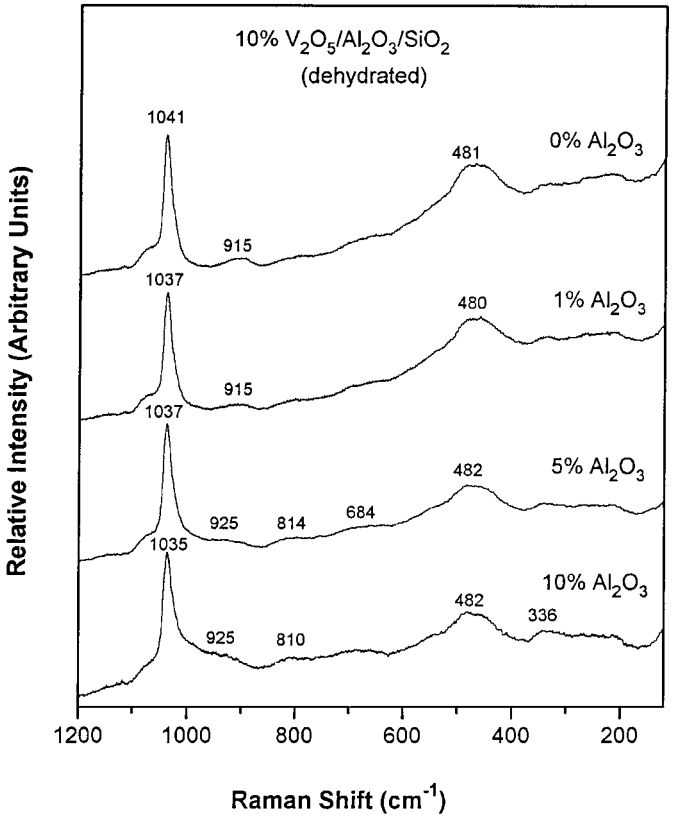

FIG. 3. Raman spectra of the dehydrated 10% $V_2O_5/Al_2O_3/SiO_2$ samples.

not certain whether the broad, weak Raman band at 915–925 cm^{-1} for the 10% V_2O_5/10% Al_2O_3/SiO_2 catalyst is due to a minor amount of the surface polymeric vanadia species or due to the same isolated VO_4 species with the VO_3 vibration becoming slightly more Raman active in association with the modification of silica by aluminum oxide species. In any case, the similarity between the Raman spectra of the dehydrated 10% $V_2O_5/Al_2O_3/SiO_2$ and 10% V_2O_5/SiO_2 samples indicates that the isolated VO_4 species are the dominant surface vanadium oxide species on the Al_2O_3/SiO_2 supports.

3. UV–Vis-NIR Diffuse Reflectance Spectroscopy

The NIR DRS spectra of the dehydrated SiO_2, Al_2O_3/SiO_2, and $V_2O_5/Al_2O_3/SiO_2$ samples are compared in Fig. 4. In the NIR region where the combination band and overtone vibrations of O–H groups are located, the 7315-cm^{-1} band due to the isolated Si–OH hydroxyls (15) decreases with increasing alumina loading, indicating that the deposition of aluminum oxide species consumes the surface Si–OH groups, in agreement with the Raman results. However, the absorption band due to the Al–OH hydroxyls is not visible due to the strong 7315-cm^{-1} band. Upon deposition of the surface vanadium oxide species on the

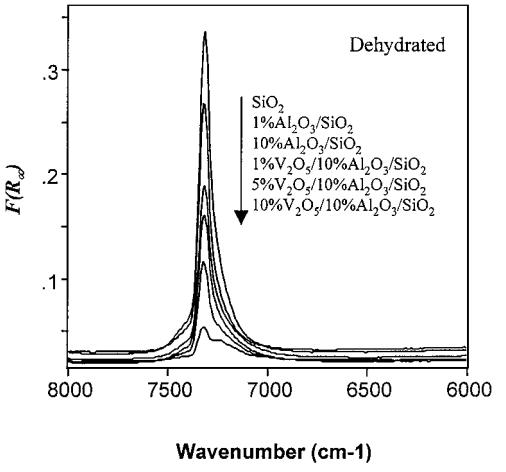

FIG. 4. NIR DRS spectra of the dehydrated Al_2O_3/SiO_2 and $V_2O_5/Al_2O_3/SiO_2$ samples.

Al_2O_3/SiO_2 supports, the intensity of the 7315-cm^{-1} band further decreases (see also Fig. 4), indicative of the interaction between surface vanadium oxide species and the silica surface.

The UV–vis DRS spectra of the dehydrated 5% V_2O_5 on SiO_2, Al_2O_3/SiO_2, and Al_2O_3 supports are compared in Fig. 5, and their band maxima and edge energies are provided in Table 2. No apparent absorption in the UV–vis region is observed for the Al_2O_3/SiO_2 samples (not shown here). The UV–vis DRS spectra of the dehydrated 5% $V_2O_5/Al_2O_3/SiO_2$ samples display only one ligand-to-metal charge transfer (LMCT) band at 280–271 nm due to electronic transitions from orbitals mainly consisting of oxygen 2*p* orbitals to vanadium 3*d* orbitals (13). These spectra are very similar to the dehydrated 5% V_2O_5/SiO_2, and their edge energies are about the same (3.5–3.6 eV). These results strongly suggest that the dehydrated surface vanadium

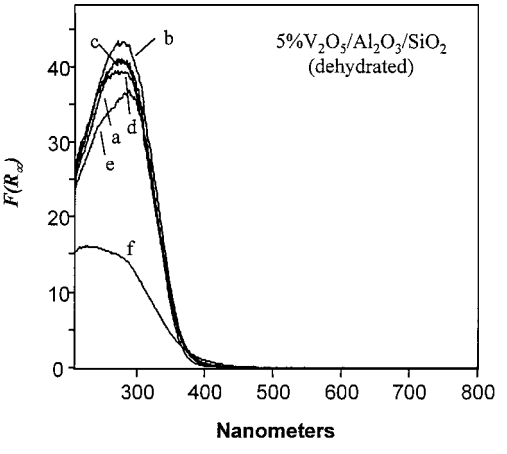

FIG. 5. UV–vis DRS spectra of the dehydrated samples: (a) 5% V_2O_5/SiO_2; (b) 5% V_2O_5/1% Al_2O_3/SiO_2; (c) 5% V_2O_5/3% Al_2O_3/SiO_2; (d) 5% V_2O_5/5% Al_2O_3/SiO_2; (e) 5% V_2O_5/10% Al_2O_3/SiO_2; (f) 5% V_2O_5/Al_2O_3.

TABLE 2

Band Maxima and Edge Energies of the $V_2O_5/Al_2O_3/SiO_2$ Samples under Hydrated and Dehydrated Conditions

Sample	Band max.[a] (nm) (dehy)	E_g (eV) (dehy)	Band max.[a] (nm) (hydr)	E_g (eV) (hydr)
1% V_2O_5/10% Al_2O_3/SiO_2	254	3.8	261	3.7
1% V_2O_5/Al_2O_3	236	3.9	252	3.9
5% V_2O_5/SiO_2	286	3.5	285, 433	2.4
5% V_2O_5/1% Al_2O_3/SiO_2	277	3.6	277, 401 (sh)	2.7
5% V_2O_5/3% Al_2O_3/SiO_2	274	3.6	276, 397 (sh)	3.3
5% V_2O_5/5% Al_2O_3/SiO_2	271	3.6	274, 390 (sh)	3.4
5% V_2O_5/10% Al_2O_3/SiO_2	280	3.6	278	3.5
5% V_2O_5/Al_2O_3	241	3.7	256	3.7
10% V_2O_5/10% Al_2O_3/SiO_2	284	3.5	281, 398 (sh)	3.4
10% V_2O_5/Al_2O_3	263	3.3	266	3.3

[a] The band maximum values are obtained by curve fitting.

oxide species on Al_2O_3/SiO_2 supports are predominantly isolated VO_4 species, similar to the dehydrated V_2O_5/SiO_2 (13). The edge position of the dehydrated 5% V_2O_5/Al_2O_3 sample is located at ~3.7 eV with a broad band centered at ~241 nm (see Table 2), suggesting that the surface vanadium oxide species on pure alumina at 5% V_2O_5 loading is predominantly isolated VO_4 species, in agreement with the literature results (14, 16). Furthermore, the edge energy of the isolated VO_4 species on Al_2O_3 is ~0.2–0.3 eV higher than that on SiO_2. The change of the support appears to affect the edge energy of the surface vanadium oxide species.

The UV–vis DRS spectra of the hydrated 5% V_2O_5 on SiO_2, Al_2O_3/SiO_2, and Al_2O_3 supports are compared in Fig. 6 and their band maxima and edge energies are also listed in Table 2. The hydrated 5% V_2O_5/SiO_2 sample exhibits two major LMCT bands at 285 and 433 nm with an edge energy of 2.4 eV due to polymerized VO_5/VO_6

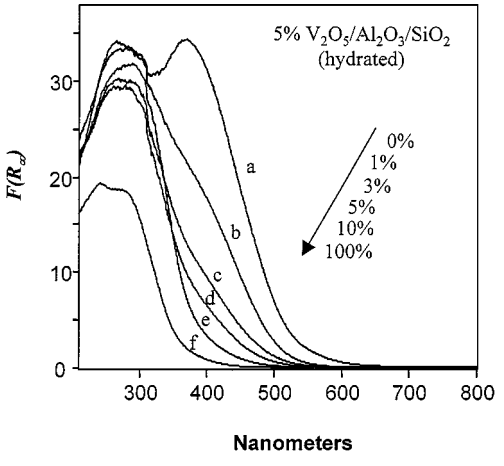

FIG. 6. UV–vis DRS spectra of the hydrated samples (a) 5% V_2O_5/SiO_2; (b) 5% V_2O_5/1% Al_2O_3/SiO_2; (c) 5% V_2O_5/3% Al_2O_3/SiO_2; (d) 5% V_2O_5/5% Al_2O_3/SiO_2; (e) 5% V_2O_5/10% Al_2O_3/SiO_2; (f) 5% V_2O_5/Al_2O_3.

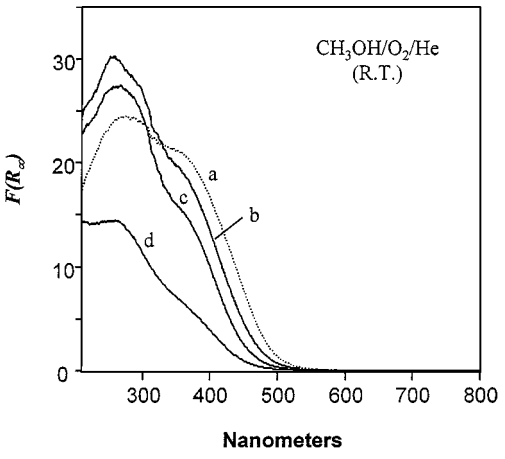

FIG. 7. UV–vis DRS spectra of samples after $CH_3OH/O_2/He$ at r.t.: (a) 5% V_2O_5/SiO_2; (b) 5% V_2O_5/3% Al_2O_3/SiO_2; (c) 5% V_2O_5/10% Al_2O_3/SiO_2; (d) 5% V_2O_5/Al_2O_3.

species (13). Modification of silica by surface aluminum oxide species dramatically reduces the intensity of the second LMCT band with a longer wavelength. Simultaneously, the edge energy of the LMCT transitions of the V cations markedly increases, indicative of a decrease in the average polymerization degree of surface vanadium oxide species due to the presence of the more basic aluminum oxide species (17). The edge energy of the hydrated 5% V_2O_5/10% Al_2O_3/SiO_2 sample is 3.5 eV, which is very close to that of the hydrated 5% V_2O_5/Al_2O_3 sample (see Table 2). These UV–vis DRS measurements demonstrate that the molecular structure of the hydrated surface vanadium oxide species on Al_2O_3/SiO_2 is very similar to that on pure Al_2O_3 rather than on pure SiO_2 at high surface alumina coverages.

The UV–vis DRS spectra of the 5% V_2O_5 on SiO_2, Al_2O_3/SiO_2, and Al_2O_3 supports after methanol chemisorption at room temperature are compared in Fig. 7, and the corresponding band maxima and edge energies are presented in Table 3. Two LMCT bands are observed at 252–266 and 369–389 nm for these samples. The edge position of the 5% V_2O_5/SiO_2 sample is located at 2.7 eV, which is due

TABLE 3

Band Maxima and Edge Energies of the 5% $V_2O_5/Al_2O_3/SiO_2$ Samples after $CH_3OH/O_2/He$ Adsorption at Room Temperature and 120°C

Sample	Band max.[a] (nm) (r.t.)	E_g (eV) (r.t.)	Band max.[a] (nm) (120°C)	E_g (eV) (120°C)
5% V_2O_5/SiO_2	263, 389	2.7	—	—
5% V_2O_5/3% Al_2O_3/SiO_2	261, 388	2.8	253, 380 (sh)	3.5
5% V_2O_5/10% Al_2O_3/SiO_2	266, 378	2.9	264, 380 (sh)	3.6
5% V_2O_5/Al_2O_3	252, 369	3.6	253, 384 (sh)	3.6

[a] The band maximum values are obtained by curve fitting.

to the polymerized VO_5/VO_6 methoxy species on the silica surface (13). Only a slight increase in the edge energy is observed with the addition of the aluminum oxide species, suggesting that a similar type of polymerized VO_5/VO_6 methoxy species are present on the Al_2O_3/SiO_2 surface after methanol chemisorption at room temperature. At a higher chemisorption temperature of 120°C, the relative intensity of the second LMCT band at lower wavenumber dramatically decreases and the edge position increases to 3.5–3.6 eV, suggesting that the surface vanadium oxide/methoxy species are predominantly isolated VO_4 units (13). In contrast, the edge energy of the 5% V_2O_5/Al_2O_3 sample after methanol chemisorption at room temperature as well as at 120°C is almost the same as that of the dehydrated sample (the slight decrease of 0.1 eV may be due to the change of Al(III)–O^- and/or H–O^- ligands to methoxy ligands). These results indicate that the average polymerization degree of surface vanadium oxide species on the 5% V_2O_5/Al_2O_3 sample is not significantly affected by the environmental conditions.

4. *Temperature-Programmed Reduction (TPR)*

The TPR spectra of 1% V_2O_5 on SiO_2, 1–10% Al_2O_3/SiO_2, and Al_2O_3 supports are shown in Fig. 8, and the corresponding TPR results are listed in Table 4. It can be seen that the maximum reduction temperature (T_{max}) of the 1% V_2O_5/Al_2O_3 sample is significantly higher than that of 1% V_2O_5/SiO_2, and its peak width is significantly broader than the latter. However, their initial reduction temperatures (T_{onset}) appear to occur at very similar temperatures, considering the relatively low signal-to-noise ratio at this low vanadia loading. The T_{max} and peak width of the 1% $V_2O_5/Al_2O_3/SiO_2$ catalysts increase systematically with the alumina content. These results demonstrate that the reduction behavior of the surface vanadium oxide species on Al_2O_3/SiO_2 approaches that of V_2O_5/Al_2O_3 with increasing alumina content, suggesting an increasing interaction between surface vanadium oxide and aluminum oxide species on silica at high surface alumina coverages.

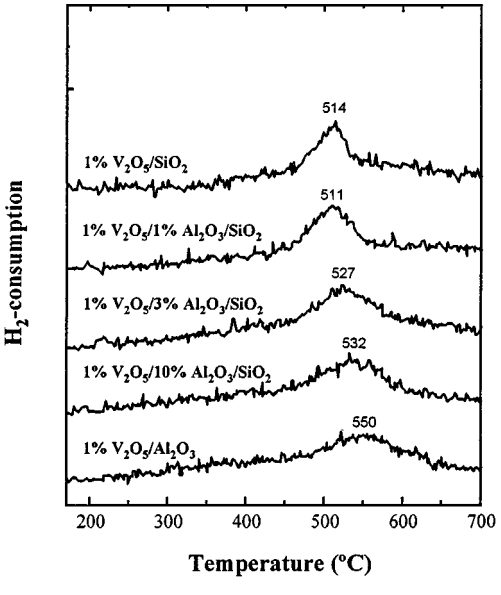

FIG. 8. TPR profiles of 1% V_2O_5 on SiO_2, Al_2O_3/SiO_2, and Al_2O_3 supports.

TABLE 4

TPR Results for 1% V_2O_5 on SiO_2, Al_2O_3, and Al_2O_3/SiO_2 Supports

Sample	T_{onset} (°C)	T_{max} (°C)	FWHM (°C)[a]	H/V (atomic ratio)
1% V_2O_5/SiO_2	396	514	40	1.87
1% V_2O_5/1% Al_2O_3/SiO_2	400	511	58	1.91
1% V_2O_5/3% Al_2O_3/SiO_2	400	527	82	2.12
1% V_2O_5/10% Al_2O_3/SiO_2	400	532	94	2.11
1% V_2O_5/Al_2O_3	404	550	102	1.94

[a] The peak width at the half-peak intensity.

The TPR results and spectra of 5% V_2O_5 on SiO_2, 1–10% Al_2O_3/SiO_2, and Al_2O_3 supports are presented in Table 5 and Fig. 9. In this case, the T_{max} and T_{onset} of 5% V_2O_5/Al_2O_3 are lower than those of 5% V_2O_5/SiO_2, whereas its peak width is still much larger than that of 5% V_2O_5/SiO_2. The T_{max} of the 5% $V_2O_5/Al_2O_3/SiO_2$ catalysts decreases but their peak width increases systematically with increasing alumina content. Similar results are obtained for the 10% $V_2O_5/Al_2O_3/SiO_2$ catalysts and are shown in Table 6. The TPR results indicate that the surface aluminum oxide species on silica modify the reduction behavior of the surface vanadium oxide species to approach that of V_2O_5/Al_2O_3. Thus, the TPR results suggest an intimate interaction between surface vanadium oxide and aluminum oxide species on silica.

The H/V ratios for 1–10% V_2O_5 loadings on SiO_2 and Al_2O_3/SiO_2 supports are almost constant at ~2 (see Tables 4–6), indicating that the average oxidation state of

TABLE 5

TPR Results for 5% V_2O_5 on SiO_2, Al_2O_3, and Al_2O_3/SiO_2 Supports

Sample	T_{onset} (°C)	T_{max} (°C)	FWHM (°C)	H/V (atomic ratio)
5% V_2O_5/SiO_2	383	526	40	1.88
reoxidized	386	534	39	1.90
5% V_2O_5/1% Al_2O_3/SiO_2	391	523	50	2.08
reoxidized	400	533	50	2.06
5% V_2O_5/5% Al_2O_3/SiO_2	374	520	60	2.13
reoxidized	382	531	66	2.14
5% V_2O_5/10% Al_2O_3/SiO_2	368	518	76	2.08
reoxidized	377	530	79	2.08
5% V_2O_5/Al_2O_3	313	493	78	1.75
reoxidized	312	496	133	1.53

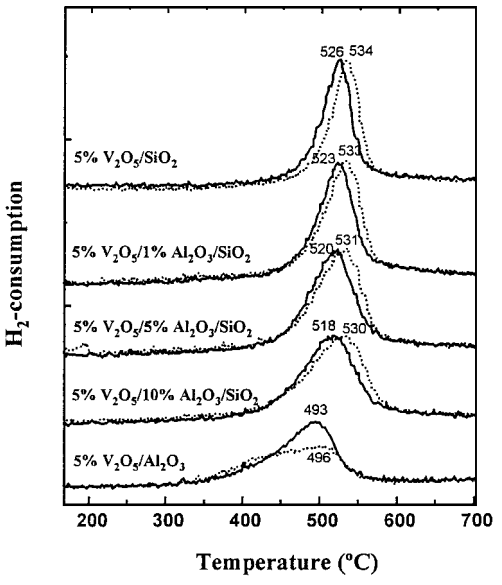

FIG. 9. Comparison of TPR profiles of fresh (solid lines) and reoxidized (dotted lines) samples.

the V cations on these supports after the TPR runs up to 700°C is about +3. However, the H/V ratios for 5% and 10% V_2O_5/Al_2O_3 are 1.75 and 1.66, respectively, which are out of the experimental error range of 10%. The Al_2O_3 support was found to be able to stabilize the V^{4+} oxidation state (18), while no literature results were found to support the stabilization of V^{3+} after reoxidizing the reduced catalysts. It would appear that some V^{4+} cations are stabilized on pure alumina, giving rise to an average oxidation state higher than +3 in the present work. This is further supported by the comparison of the TPR results of the fresh and reoxidized samples of 5% V_2O_5 on SiO_2, 1–10% Al_2O_3/SiO_2, and Al_2O_3 supports; see Table 5 and Fig. 9. The H/V ratio of the reoxidized 5% V_2O_5/Al_2O_3 sample becomes even lower than that of the fresh sample, indicating that more V^{4+} cations are stabilized on alumina during the second TPR run. In addition, the reduction peak width of the reoxidized 5% V_2O_5/Al_2O_3 sample becomes remarkably broad, demonstrating that its surface is much more heterogeneous than the fresh sample. In contrast, the H/V ratios as well as the peak shape of the reoxidized 5% V_2O_5/SiO_2 and 5% $V_2O_5/Al_2O_3/SiO_2$ samples are fairly similar to the fresh samples, indicating that the surface vanadium oxide species on SiO_2 and Al_2O_3/SiO_2 supports are much more stable after the redox cycle.

TABLE 6

TPR Results for 10% V_2O_5 on SiO_2, Al_2O_3, and Al_2O_3/SiO_2 Supports

Sample	T_{onset} (°C)	T_{max} (°C)	FWHM (°C)	H/V (atomic ratio)
10% V_2O_5/SiO_2	390	540	38	2.00
10% V_2O_5/1% Al_2O_3/SiO_2	387	537	42	2.04
10% V_2O_5/5% Al_2O_3/SiO_2	383	530	53	2.04
10% V_2O_5/10% Al_2O_3/SiO_2	357	528	61	2.11
10% V_2O_5/Al_2O_3	296	493	82	1.66

5. *Methanol Oxidation*

Methanol oxidation was used to examine the catalytic properties of the Al_2O_3/SiO_2 and $V_2O_5/Al_2O_3/SiO_2$ catalysts, and their catalytic results for methanol oxidation at 270°C are presented in Table 7. The silica support did not show any noticeable activity for methanol oxidation under the present experimental conditions. Pure Al_2O_3 and Al_2O_3/SiO_2 produce exclusively the dehydration product (dimethyl ether), indicating that the active sites in the catalytic materials for methanol oxidation are all acid sites (19). By assuming that all the Al cations are molecularly dispersed on the silica surface (as suggested by the XPS experiments), the turnover frequencies (TOF_{dehy}) of the Al_2O_3/SiO_2 samples for methanol dehydration can be calculated. The TOF_{dehy} slightly decreases with increasing alumina loading. However, it is not clear whether the active sites on Al_2O_3/SiO_2 are Lewis or Brönsted acid sites, and acidity characterization of these materials is still continuing.

Interestingly, the addition of vanadium oxide onto the 1–10% Al_2O_3/SiO_2 supports does not affect their TOF_{dehy} values, irrespective of the vanadia loading, indicating that the acid sites are not affected by the presence of the V cations. On the other hand, the activity for the redox products (formaldehyde, methyl formate, and dimethoxy methane) on the $V_2O_5/Al_2O_3/SiO_2$ catalysts is noticeably enhanced relative to the V_2O_5/SiO_2 catalyst. The TOF_{redox} of the 1% V_2O_5/1% Al_2O_3/SiO_2 catalyst is over an order of magnitude higher than that of the 1% V_2O_5/SiO_2 catalyst, indicating that the surface vanadium oxide species directly interact with the aluminum oxide species. Increasing the alumina content slightly increases the TOF_{redox} of the 1% $V_2O_5/Al_2O_3/SiO_2$ catalysts, which is comparable to that of the V_2O_5/Al_2O_3 catalysts. However, increasing the vanadia content on the Al_2O_3/SiO_2 support generally decreases the TOF_{redox}, which is indicative of the decreased average interaction between surface vanadium oxide and aluminum oxide species (averaged for each V cation). In the case that the V/Al atomic ratio is around 1 or higher (e.g., 1% V_2O_5/1–10% Al_2O_3/SiO_2 and 5% V_2O_5/5–10% Al_2O_3/SiO_2 catalysts), their TOF_{redox} is over an order of magnitude higher than that of the V_2O_5/SiO_2 catalyst and is comparable to that of the V_2O_5/Al_2O_3 catalyst. These interesting results point out that the $V_2O_5/Al_2O_3/SiO_2$ catalysts possess two types of surface-active sites, i.e., the acid sites that are associated with surface aluminum oxide species and the redox sites of the surface V cations that are in direct interaction with the surface aluminum oxide species. These two types of sites

TABLE 7

Reactivity and Selectivity of Al_2O_3/SiO_2 and $V_2O_5/Al_2O_3/SiO_2$ Catalysts for Methanol Oxidation at 270°C

Catalyst	A_c[a] (mmol/g · h)	TOF_{redox}[b] (10^{-3} s^{-1})	TOF_{dehy}[c] (10^{-3} s^{-1})	Selectivity (%)			
				HCHO	MF	DMM	DME
1% Al_2O_3/SiO_2	24	—	34	—	—	—	100
3% Al_2O_3/SiO_2	38	—	18	—	—	—	100
5% Al_2O_3/SiO_2	56	—	16	—	—	—	100
10% Al_2O_3/SiO_2	67	—	10	—	—	—	100
Al_2O_3	563	—	—	—	—	—	100
1% V_2O_5/SiO_2	1	2	—	—	—	—	—
1% V_2O_5/1% Al_2O_3/SiO_2	31	35	24	31	11	3	55
1% V_2O_5/5% Al_2O_3/SiO_2	68	52	14	25	4	1	70
1% V_2O_5/10% Al_2O_3/SiO_2	78	55	8	23	3	2	72
5% V_2O_5/1% Al_2O_3/SiO_2	40	9	34	34	4	4	58
5% V_2O_5/5% Al_2O_3/SiO_2	86	19	15	38	3	2	57
5% V_2O_5/10% Al_2O_3/SiO_2	106	24	9	39	4	2	55
10% V_2O_5/5% Al_2O_3/SiO_2	86	9	15	38	2	3	57
10% V_2O_5/10% Al_2O_3/SiO_2	102	13	8	46	2	3	49
10% V_2O_5/Al_2O_3	430	34	—	31	1	2	66

[a] Millimoles of methanol converted per gram of catalyst per hour.

[b] TOF_{redox} is calculated on the basis of the total V atoms in the catalysts for the production of HCHO + MF (methyl formate) + DMM (dimethoxy methane).

[c] TOF_{dehy} is calculated on the basis of the total Al atoms in the catalysts for the production of dimethyl ether (DME).

appear to work independently to convert methanol to different products.

DISCUSSION

The presence of the Si–O–Al bonds in the mixed Al_2O_3/SiO_2 thin film prepared by annealing the deposited Al on a SiO_2 thin film has been reported by Grundling *et al.* (21). They found that this mixed Al_2O_3/SiO_2 thin film exhibits electronic properties similar to those of bulk aluminosilicates. Sato *et al.* (6) reported that the deposition of silica on alumina by chemical vapor deposition (CVD) convert all Lewis acid sites on alumina to Brönsted acid sites. The presence of Brönsted acidity on the silica monolayer on alumina has also been reported by Niwa *et al.* (8), who proposed that the Brönsted acid sites are Al–O–SiOH species in the Si–O–Si network on the alumina surface. Sheng and Gay (7) further confirmed the presence of the Al–O–Si connections and Al–O–SiOH or Al–O–$(SiO)_n$–SiOH groups on the silica-modified alumina monolayer catalyst by combined IR and ^{29}Si MAS NMR techniques.

In the present study, a highly reactive H-sequestering reagent of Al *sec*-butoxide was used as the precursor to prepare the highly dispersed Al_2O_3/SiO_2 supported oxides. It is expected that the Al *sec*-butoxide precursor molecules would react readily with the Si–OH groups to anchor each precursor molecule, which is common for most H-sequestering reagents during the surface reaction with silica (10). The consumption of the Si–OH hydroxyls by deposition of aluminum oxide species on silica is confirmed by both Raman and NIR DRS spectroscopy. Thus, the Si–O–Al bonds should be formed on the silica surface after deposition of the aluminum oxide species. The XPS surface analysis demonstrates that the Al/Si atomic ratio correlates linearly with the alumina content up to 10% Al_2O_3, which suggests that the aluminum oxide species on silica are most likely highly dispersed. The BE values of Al 2*p* for these Al_2O_3/SiO_2 samples are between 75.1 and 74.8 eV, which are essentially independent of the alumina loading within experimental error (±0.2 eV). This is similar to the XPS results of the mixed Al_2O_3/SiO_2 thin films where the BE of Al 2*p* remains constant over a wide range of film composition (21). However, the local structure of the Al cations and nature of chemical connections between Si and Al cations (e.g., Si–O–Al–OH and Si–OH–Al) are not clear at the present time since detailed ^{29}Si NMR and FT-IR characterization experiments were not performed.

With the Al_2O_3/SiO_2 supported oxides as support materials, the deposition of the vanadium oxide species is expected to consume surface hydroxyl groups of Al–OH and/or Si–OH. The consumption of some Si–OH hydroxyls is confirmed by NIR DRS results. The fact that the Al–OH hydroxyls are not identified by the NIR DRS spectra because of their low concentrations cannot exclude their presence on Al_3O_2/SiO_2 catalysts. Some of the Al–OH hydroxyls may be formed from the hydrolysis of the Al–O–Si bonds, as in the case of the other silica-supported surface metal oxides (e.g., TiO_2/SiO_2 and ZrO_2/SiO_2) (15, 22). On the pure alumina surface, the ratio of the Lewis acid sites (Al^{3+}) to Al–OH sites is a strong function of pretreatment

temperature (23) and is zero at a pretreatment temperature of 150°C or lower. The deposition of vanadium oxide on alumina at room temperature consumes only the Al–OH hydroxyls in a sequential fashion from the most basic OH groups to the neutral OH groups and further to the most acidic OH groups (24). In a similar manner, the deposition of vanadium oxide species on Al_2O_3/SiO_2 most likely consumes first the Al–OH hydroxyls, even at a relatively low concentration on the surface since these hydroxyls may be more reactive than the Si–OH hydroxyls. This occurs because the Al–OH hydroxyls are more basic than the Si–OH hydroxyls since the Al(III) cations are less electronegative than the Si(IV) cations (25), as evidenced also from the higher net surface pH at point-of-zero charge (pzc) of alumina relative to silica (17). Therefore, the consumption of Al–OH as well as Si–OH hydroxyls would result in the coexistence of Al–O–V and Si–O–V bridging bonds in this bilayered catalyst system.

In situ Raman spectroscopy and UV–vis-NIR DRS show that the molecular structures of the $V_2O_5/Al_2O_3/SiO_2$ samples are a strong function of environmental conditions. In the dehydrated state, the Raman spectra of the $V_2O_5/Al_2O_3/SiO_2$ samples are very similar to those of the highly dispersed V_2O_5/SiO_2 samples. In addition, the spectral features and edge energies of the $V_2O_5/Al_2O_3/SiO_2$ samples are very close to those of the highly dispersed V_2O_5/SiO_2 samples. These results suggest that the dehydrated surface vanadium oxide species on the Al_2O_3/SiO_2 supports are predominantly isolated VO_4 units (i.e., $O{=}V(O{-}Support)_3$).

In the hydrated state, the UV–vis DRS results indicate that the molecular structure of the surface vanadium oxide species on the Al_2O_3/SiO_2 supports is a strong function of the alumina and vanadia loadings. The presence of the aluminum oxide species significantly decreases the polymerization degree of the hydrated surface vanadium oxide species relative to the highly polymerized VO_5/VO_6 on pure SiO_2. The similarity of the UV–vis DRS spectral feature and edge energy of the hydrated surface vanadium oxide species on 10% Al_2O_3/SiO_2 and pure Al_2O_3 indicates that the molecular structure of the hydrated surface vanadium oxide species on Al_2O_3/SiO_2 is similar to the structure present in V_2O_5/Al_2O_3 rather than in V_2O_5/SiO_2 at higher surface alumina coverages. For the hydrated V_2O_5/Al_2O_3 samples, the edge energy decreases as the vanadia loading increases from 1% to 10% V_2O_5, which may be associated with the increase in the polymerization degree of vanadium oxide species (13). The high E_g value of 3.9 eV for the hydrated 1% V_2O_5/Al_2O_3 sample indicates the presence of isolated VO_4 species, which is probably $VO_3(OH)$ species (16). For the hydrated 5% V_2O_5/Al_2O_3 sample, a small amount of polymerized metavanadate species $(VO_3)_n$ may be present in addition to the $VO_3(OH)$ species due to the decrease of the edge energy. In the case of the hydrated 10% V_2O_5/Al_2O_3 sample, Raman and solid-state ^{51}V NMR spectroscopy detected the presence of decavanadate ($V_{10}O_{28}$)-like clusters (16), which account for the further decrease in the edge energy of the surface vanadium oxide species.

The previous discussion suggests that, under hydrated conditions, the presence of the surface aluminum oxide species on silica significantly modifies the molecular structure of the surface vanadium oxide species and changes their hydrated molecular structure from VO_5/VO_6 polymers to less polymerized metavandate $(VO_3)_n$ species and/or isolated $VO_3(OH)$ species, which depend on the relative amount of alumina and vanadia on the silica surface. The high-alumina and low-vanadia loadings (e.g., 1% V_2O_5/10% Al_2O_3/SiO_2) gives rise to predominantly isolated $VO_3(OH)$ species, whereas low-alumina and high-vanadia loadings (e.g., 5% V_2O_5/1% Al_2O_3/SiO_2) result in mainly polymerized VO_5/VO_6 species. It has been shown (17) that the structure of the hydrated surface vanadium oxide overlayer follows the V(V) aqueous chemistry as a function of net pH at pzc. Therefore, the addition of the more basic aluminum oxide species should increase the net surface pH at pzc relative to silica and decrease the polymerization degree of the vanadium oxide species. However, under methanol saturation conditions, the UV–vis results indicate that the molecular structure of the surface vanadium methoxy species on Al_2O_3/SiO_2, like that on pure SiO_2, is highly polymerized VO_5/VO_6 methoxy species (13), and is independent of the alumina loading. Thus, the polymerization degree of surface vanadium methoxy species is independent of the net surface pH on Al_2O_3/SiO_2 under methanol saturation conditions. This result also further confirms that the molecular structure of the dehydrated surface vanadium oxide species on Al_2O_3/SiO_2, like that on SiO_2, are isolated VO_4 units with V–O–Support bridging bonds that are readily broken upon the chemisorption of methanol to form highly polymerized $V{-}OCH_3{-}V$ methoxy species (13). In the following discussion, only the dehydrated molecular structures of the $V_2O_5/Al_2O_3/SiO_2$ catalysts are addressed since the catalysts are usually operated in the dehydrated state during methanol oxidation as well as the TPR studies.

The TPR results indicate that the reduction behavior of the $V_2O_5/Al_2O_3/SiO_2$ catalysts is a strong function of the alumina loading. The higher the alumina loading on the $V_2O_5/Al_2O_3/SiO_2$ catalysts, the closer the TPR values (T_{max}, T_{onset}, and peak width) to those of the V_2O_5/Al_2O_3 catalysts. The aluminum oxide species on silica appears to strongly modify the chemical properties of the surface vanadium oxide species, suggesting an intimate interaction between these two species.

Even far below the monolayer coverage for either vanadium oxide or aluminum oxide on silica, the addition of 1% V_2O_5 onto the 1% Al_2O_3/SiO_2 sample greatly enhances the

redox reactivity (over 10 times) for methanol oxidation relative to 1% V_2O_5/SiO_2. This result suggests a direct interaction between the surface vanadium oxide and aluminum oxide species (i.e., the formation of V–O–Al connections) and indicates that the V(V) cations are preferentially coordinated to the surface aluminum oxide species. This fact confirms the previous suggestion that the deposition of vanadium oxide species on Al_2O_3/SiO_2 preferentially consumes the surface Al–OH hydroxyls to form V–O–Al bonds since these hydroxyls may be more basic and reactive than the Si–OH hydroxyls.

Although the surface structure of the highly dispersed $V_2O_5/Al_2O_3/SiO_2$ catalysts in the dehydrated state is pretty much the same as that of the highly dispersed V_2O_5/SiO_2 catalysts, the modification of the silica support by the surface aluminum oxide species greatly affects the catalytic properties of the supported vanadium oxide species. The TOF_{redox} for methanol oxidation on the highly dispersed $V_2O_5/Al_2O_3/SiO_2$ catalysts increases by more than an order of magnitude relative to the V_2O_5/SiO_2 catalysts and are comparable to that of the V_2O_5/Al_2O_3 catalysts. The replacement of the Si(IV)–O^- ligand by the Al(III)–O^- ligand in the coordination sphere of the V cation must be responsible for the enhanced reactivity of the surface V active sites since the structure of the dehydrated surface vanadium oxide species of these catalysts consists of isolated O=V(O–Support)$_3$ groups. The basis for this support effect may lie in the increase of the electron density of the bridging oxygen of the V–O–Support bond due to the formation of V–O–Al bridging bonds since the Al(III) cations possess a lower electronegativity than the Si(IV) cations (25).

Another interesting observation for the $V_2O_5/Al_2O_3/SiO_2$ catalyst system is that the TOF_{dehy} values for methanol dehydration are almost the same as those of the Al_2O_3/SiO_2 supports at the same alumina loading. This suggests that the acid sites are not the binding sites for anchoring the V cations and that the acid sites are most likely separated from the redox sites. This is a different behavior than that on pure Al_2O_3, where the deposition of surface vanadium oxide species titrates the surface acid sites (20). On the other hand, the significant increase in the TOF_{redox} of the V cations on the Al_2O_3/SiO_2 supports relative to that of V_2O_5/SiO_2 demonstrates that the V cations directly interact with the aluminum oxide species. Thus, the catalytic results suggest that the V cations form V–O–Al bridging bonds via the chemical reaction probably with surface Al–OH hydroxyls, leaving the acid sites (e.g., Al–OH–Si) untouched, which continue to function for methanol dehydration. This also suggests that the Si–O–Al–OH sites may not be the acid sites for the methanol dehydration reaction since the consumption of the Al–OH hydroxyls by the vanadium oxide species does not affect the acid reactivity. Thus, it is proposed that the Si–OH–Al bridging bonds on silica are most likely the acid sites that are responsible for methanol dehydration with or without the presence of the V cations.

CONCLUSIONS

In situ Raman and UV–vis-NIR DR spectroscopic studies of the highly dispersed $V_2O_5/Al_2O_3/SiO_2$ catalysts demonstrate that the surface vanadium oxide species are predominantly isolated VO_4 units in the dehydrated state. Upon hydration, the molecular structure of the surface vanadium oxide species on Al_2O_3/SiO_2 is determined by the net pH at pzc and is a strong function of alumina and vanadia loadings, ranging from polymerized VO_5/VO_6 species at low-alumina and high-vanadia loadings, similar to pure silica, to isolated $VO_3(OH)$ and polymerized metavanadate $(VO_3)_n$ species at high-alumina and low-vanadia loadings, similar to pure alumina. Under methanol saturation conditions, however, the surface structure of the $V_2O_5/Al_2O_3/SiO_2$ catalysts is independent of the alumina and vanadia loadings and consists of highly polymerized VO_5/VO_6 methoxy species. The surface V cations preferentially interact with the surface aluminum oxide species on silica, possibly due to the more reactive Al–OH hydroxyls on Al_2O_3/SiO_2 relative to the Si–OH hydroxyls. Consequently, the reducibility and catalytic properties of the surface vanadium oxide species are significantly altered. The TOF_{redox} of the surface VO_4 species on Al_2O_3/SiO_2 supports for methanol oxidation increases by more than an order of magnitude relative to the V_2O_5/SiO_2 catalysts, which are comparable to the reactivity of the V_2O_5/Al_2O_3 catalysts. It is concluded that the replacement of Si(IV)–O^- oxygenated ligands by less electronegative Al(III)–O^- ligands around the V cations are responsible for the enhanced reactivity of the V sites. Interestingly, the reactivity of the acid sites (TOF_{dehy}) on the $V_2O_5/Al_2O_3/SiO_2$ catalysts is not affected by the presence of the vanadium oxide species, which suggests that the active acid sites on Al_2O_3/SiO_2 are probably located at the Si–OH–Al bonds.

ACKNOWLEDGMENTS

This work was funded by the U.S. National Science Foundation, Grant CTS-9417981. The UV–vis-NIR DRS experiments were performed on a Varian Cary 5 UV–vis-NIR spectrometer that was supported by the U.S. Department of Energy—Basic Energy Sciences, Grant DE-FG02-93ER14350. The authors would like to thank Dr. J. L. G. Fierro for XPS analysis and Dr. Miguel A. Banares for BET measurements.

REFERENCES

1. Corma, A., *Chem. Rev.* **95**, 559 (1995).
2. Reddy, B. N., and Subrahmanyam, M., *Langmuir* **8**, 2072 (1992).
3. Ahlstrom-Silversand, A. F., and Odenbrand, C. U. I., *Appl. Catal.* **153**, 157 (1997).
4. Rajagopal, S., Grimm, T. L., Collins, D. J., and Miranda, R., *J. Catal.* **137**, 453 (1992), and references cited therein.

5. (a) Kiessling, D., Went, G., Hagenau, K., and Schoellner, R., *Appl. Catal.* **71**, 69 (1991); (b) Kiessling, D., and Froment, G. F., *Appl. Catal.* **71**, 123 (1991).
6. Sato, S., Toita, M., Sodesawa, T., and Nozaki, F., *Appl. Catal.* **62**, 73 (1990).
7. (a) Sheng, T.-C., and Gay, I. D., *J. Catal.* **145**, 10 (1994); (b) Sheng, T.-C., Lang, S., Morrow, B. A., and Gay, I. D., *J. Catal.* **148**, 341 (1994).
8. (a) Niwa, M., Katada, N., and Murakami, Y., *J. Phys. Chem*. **94**, 6441 (1990). (b) Katada, N., Toyama, T., Niwa, M., Tsubouchi, T., and Murakami, Y., *Res. Chem. Intermed.* **9**, 137 (1995).
9. Katada, N., Ishiguro, H., Muto, K., and Niwa, M., *Chem. Vap. Deposition* **1**, 54 (1995).
10. Vansant, E. F., Van Der Voort, P., and Vrancken, K. C., *Stud. Surf. Catal.* **93**, 1995.
11. Gao, X., Bare, S. R., Fierro, J. L. G., and Wachs, I. E., *J. Phys. Chem. B* **103**, 618 (1999).
12. (a) Tallant, D. R., Bunker, B. C., Brinker, C. J., and Balfe, C. A., *Mater. Res. Soc. Symp. Proc.* **73**, 261 (1986). (b) Stolen, R. H., and Walrafen, G. E., *J. Chem. Phys.* **64**, 2623 (1976). (c) Brinker, C. J., Tallant, D. R., Roth, E. P., and Ashley, C. S., *Mater. Res. Soc. Symp. Proc.* **61**, 387 (1986).
13. Gao, X., Bare, S. R., Weckhuysen, B. M., and Wachs, I. E., *J. Phys. Chem. B* **102**, 10842 (1998).
14. Deo, G., Ph.D. thesis, Lehigh University, Bethlehem, PA, 1992.
15. Gao, X., Bare, S. R., Fierro, J. L. G., Banares, M. A., and Wachs, I. E., *J. Phys. Chem. B* **102**, 5653 (1998).
16. Deo, G., Wachs, I. E., and Haber, J., *Crit. Rev. Surf. Chem.* **4**, 141 (1994).
17. Deo, G., and Wachs, I. E., *J. Phys. Chem*. **95**, 5889 (1991).
18. Koranne, M. M., Goodwin, J. G., Jr., and Marcelin, G., *J. Catal.* **148**, 369 (1994).
19. Tatibouët, J. M., *Appl. Catal. A: Gen.* **148**, 213 (1997).
20. Deo, G., and Wachs, I. E., *J. Catal.* **146**, 323 (1994).
21. Grundling, Ch., Lercher, J. A., and Goodman, D. W., *Surf. Sci.* **318**, 97 (1994).
22. Gao, X., Fierro, J. L. G., and Wachs, I. E., *Langmuir* **15**, 3169 (1999).
23. McFarlane, R. A., and Morrow, B. A., *J. Phys. Chem*. **92**, 5800 (1988).
24. Turek, A. M., Wachs, I. E., and DeCanio, E., *J. Phys. Chem*. **96**, 5000 (1992).
25. Sanderson, R. T., *J. Chem. Edu.* **65**, 113 (1988).